DE GRUYTER
OPEN

Copper-manganese-zinc spinels in zeolites: study of EMR spectra

**Piotr Decyk,
Andrzej B. Więckowski,
Lidia Najder-Kozdrowska,
Iveta Bilkova**

Abstract. The aim of this study is the application of electron magnetic resonance (EMR) spectroscopy to determine the interactions between NaY and HY zeolites and Cu-Mn-Zn spinels loaded onto the zeolite surfaces. The materials were characterized using XRD and IR spectroscopies. Four types of EMR lines were observed for Cu-Mn-Zn/NaY, Cu-Mn-Zn/HY samples. The difference between the EMR spectra recorded at 77 and 293 K has been shown. The spectra recorded at 77 K allowed us to distinguish between the species formed on NaY and HY zeolites. The EMR spectrum of Cu-Mn-Zn/NaY recorded at 77 K showed only one line attributed to antiferromagnetic spinels $Cu_{1.4}Mn_{1.6}O_4$ and $ZnMn_2O_4$ or/and $Cu_{0.5}Zn_{0.5}Mn_2O_4$. The spinels appeared to be more stable (more strongly attached) on HY zeolite than on NaY one. It was proved that different strength of interactions between the zeolites and Cu-Mn-Zn spinels was caused by differences in the acidity of NaY and HY zeolites.

Key words: Cu-Mn-Zn spinels • electron magnetic resonance • paramagnetic complexes • Y zeolites

P. Decyk, I. Bilkova
Faculty of Chemistry,
Adam Mickiewicz University,
6 Grunwaldzka Str., 60-780 Poznań, Poland

A. B. Więckowski✉
Institute of Physics,
Faculty of Physics and Astronomy,
University of Zielona Góra,
4a Szafrana Str., 65-516 Zielona Góra, Poland
and Institute of Molecular Physics of the Polish
Academy of Sciences,
17 Smoluchowskiego Str., 60-179 Poznań, Poland,
Tel.: +48 504 534 164,
E-mail: Andrzej.Wieckowski@vp.pl

L. Najder-Kozdrowska
Institute of Physics,
Faculty of Physics and Astronomy,
University of Zielona Góra,
4a Szafrana Str., 65-516 Zielona Góra, Poland

Introduction

Mixed oxides of copper and manganese have found many applications in laboratory and industry, e.g., in catalysis. Fierro *et al.* [1] performed the preparation and characterization of different catalysts containing Cu-Zn-Mn oxides. It has been also reported by Fei *et al.* [2, 3] that Cu-Mn-Zn oxides supported on HY zeolite are active catalysts for dimethyl ether (DME) synthesis from syngas via direct CO hydrogenation. One of components of these catalysts is the non-stoichiometric spinel $Cu_{1.4}Mn_{1.6}O_4$ beside other Cu-Mn-Zn oxides. The system applied by Fei *et al.* [3] was chosen by us for the EMR study. Padlyak *et al.* [4] have employed EPR method to study Mn^{2+} and Cu^{2+} cations in lithium and potassium-lithium tetraborate glasses.

To the best of our knowledge, spinel compounds containing copper and manganese deposited on zeolites were not studied by the use of EMR spectroscopy. Bulk spinels of various compositions have been already investigated by EMR [5, 6], but no EMR studies of zeolite-supported Cu-Zn-Mn oxides have been reported so far. It is worth mentioning that the observation of changes in EMR spectra can provide information on interactions between components of the zeolite–Cu-Zn-Mn oxide system and this study is aimed at applying EMR spectroscopy to the characterization of such interactions.

Experimental

In the present study, commercial NaY (Katalistiks) and HY zeolites have been used as supports for spinels. They were modified by copper-, manganese- and zinc-containing compounds according to the procedure given in Ref. [3]. The amount of Cu-Mn-Zn spinels on zeolites was 5 and 10 wt%. The catalysts were characterized with the use of XRD and IR spectroscopic techniques. However, the main technique applied in this study was the EMR spectroscopy.

XRD patterns were recorded on an AXS D8 Advance, Bruker diffractometer using $K\alpha$ radiation (λ = 0.154 nm) in the step scanning mode of 0.05° in the angle range between 10° and 60°.

The XRD studies were complemented by Fourier-transform infrared (FTIR) spectroscopy. Infrared spectra were recorded on a Vector 22 (Bruker) spectrometer. The pellets were prepared using the sample and KBr (1 mg and 200 mg, respectively) followed by pressing the mixture.

Surface properties of zeolites were studied by *in situ* FTIR spectroscopy of adsorbed pyridine. Self-supporting pellets of about 10 mg/cm^2 were prepared and placed into a glass cell connected to a vacuum line. FTIR spectra were recorded at 293 K. All the samples were activated at 673 K under vacuum before any characterization. Pyridine was adsorbed at 473 K and evacuated at various temperatures (473–673 K) for 30 min at each temperature. The FTIR spectra of the activated samples were subtracted from those recorded after pyridine adsorption.

The EMR measurements were carried out with an X-band EPR spectrometer type SE/X 2547 RADIOPAN. The operating microwave frequency was in the range of 8.9 GHz with a magnetic field modulation of 100 kHz. For all samples under study, the spectra were recorded at room temperature (293 K) and at liquid nitrogen temperature (77 K). Additionally, for all samples with the loading of 10 wt%, EMR spectra were recorded in the temperature range of 77–373 K.

Results and discussion

In order to distinguish which kind of zeolite surface centers participate in the interactions with spinels, pyridine adsorption on NaY and HY zeolites was performed. FTIR studies of adsorbed pyridine (Py) on NaY zeolite revealed the presence of very weak Lewis acidity coming from extralattice Na$^+$ cations (Py-Na$^+$). This acidity is characterized by the presence of the band at ~1445 cm^{-1} [7, 8]. Evacuation up to 523 K caused the disappearance of this band. On the other hand, no Brønsted acidity was detected on this zeolite, as evidenced by the absence of the band at 1549 cm^{-1}, which can be ascribed to pyridine adsorbed on Brønsted acid sites (BAS) [8] (Fig. 1A).

In the case of HY zeolite, both Brønsted and Lewis acidities were observed. The strength of acid centers on the latter zeolite was much greater than
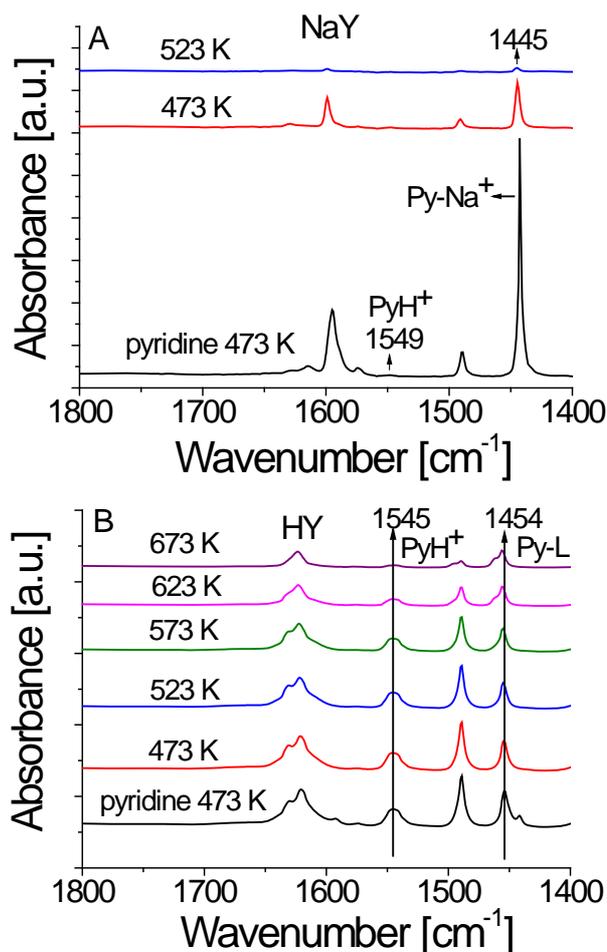
Fig. 1. FTIR spectra after pyridine adsorption and desorption in vacuum conditions at different temperatures on zeolites: A – NaY; B – HY.

that on NaY zeolite. The band at 1454 cm^{-1} originating from Lewis acidic sites (LAS) was clearly present even after evacuation at 673 K. Brønsted acid sites that formed pyridinium cations (PyH$^+$) after pyridine adsorption and gave the IR band at ~1545 cm^{-1}, as well as two other bands in the range of 1620–1640 cm^{-1} were also present (Fig. 1B).

XRD patterns and IR spectra recorded in the range of 400–1500 cm^{-1} confirmed that the crystal structure of the NaY and HY zeolites after deposition of the Cu-Mn-Zn spinels was preserved. XRD measurements have shown that beside the diffraction peaks from zeolites, additional two reflections appeared at 2θ = 35.7° and 36.4° (Fig. 2). The XRD profiles of modified zeolites Cu-Mn-Zn/NaY and Cu-Mn-Zn/HY (10 wt%) as well as the spinels calcined at 723 K were compared with those found in the database JCPDS-International Centre for Diffraction. The data permitted to assign these two reflections to Cu$_{1.4}$Mn$_{1.6}$O$_4$ and ZnMn$_2$O$_4$ or/and Cu$_{0.5}$Zn$_{0.5}$Mn$_2$O$_4$. The binary oxide Cu$_{1.4}$Mn$_{1.6}$O$_4$ (the first reflection) has a spinel structure with a cubic symmetry, the lattice constant a = 8.305 Å and the space group Fd-$3m$ (227) (PDF Card number 01-071-1145). The second reflection at 2θ = 36.4° can be attributed to ZnMn$_2$O$_4$ (hetaerolite) or/and Cu$_{0.5}$Zn$_{0.5}$Mn$_2$O$_4$, both having the spinel structure. They have tetragonal symmetry with space group
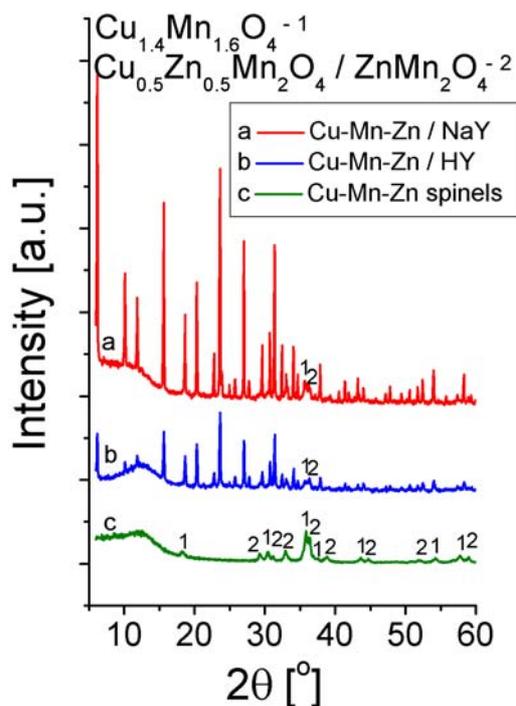
Fig. 2. XRD patterns for Cu-Mn-Zn spinels and Cu-Mn-Zn spinels loaded on NaY (10 wt%) and HY (10 wt%) zeolites.

$I41/amd$ (141) (PDF Card number 04-005-7644 and 04-007-4373). However, in this case, a direct distinction between zinc and copper-zinc-manganite is very difficult due to very similar values of network parameters $a = 5.73$ Å, $c = 9.25$ Å and $a = 5.72$ Å, $c = 9.23$ Å. The zinc and copper-zinc-manganite spinels are present in smaller amounts.

The EMR spectra of Cu-Mn-Zn spinels (10 wt%) supported on NaY and HY zeolites were characterized by the presence of four types of EMR lines:

– A very broad EMR line, the intensity of which was strongly increased and the linewidth was reduced with the decrease in temperature. We have attributed this line to the antiferromagnetic spinels $Cu_{1.4}Mn_{1.6}O_4$ and $ZnMn_2O_4$ or/and $Cu_{0.5}Zn_{0.5}Mn_2O_4$.

– A characteristic powder spectrum with anisotropy of the g factor and the hyperfine splitting a consisting of four hyperfine structure (hfs) lines, which could be attributed to a paramagnetic copper Cu^{2+} complex I (electron configuration $3d^9$, electron spin $S = \frac{1}{2}$, ground state term $^2D_{5/2}$). The hfs lines come from the interaction of the unpaired electron with the isotope ^{63}Cu nucleus (nuclear spin $I = 3/2$, abundance $A = 0.69$) and the isotope ^{65}Cu nucleus (nuclear spin

$I = 3/2$, abundance $A = 0.31$) – both isotopes having nearly equal values of nuclear magnetic moments.

– A spectrum similar to the previous one, which was assigned to another paramagnetic copper Cu^{2+} complex II.

– A nearly isotropic spectrum consisting of six hfs lines, attributed to a paramagnetic manganese Mn^{2+} complex (electron configuration $3d^5$, electron high-spin $S = 5/2$, ground state term $^6S_{5/2}$), which is characteristic of the interaction of the unpaired electron with the isotope ^{55}Mn nucleus (nuclear spin $I = 5/2$, abundance $A = 1$). These lines were observed only in the case of Cu-Mn-Zn/HY system but not in that of Cu-Mn-Zn/NaY system.

The observed EMR spectra of the two Cu^{2+} complexes can be described by the spin Hamiltonian for axial symmetry in the form:

$$\hat{H} = g_{||}\beta B_z \hat{S}_z + g_\perp \beta (B_x \hat{S}_x + B_y \hat{S}_y) + A_{||}\hat{S}_z \hat{I}_z + A_\perp (\hat{S}_x \hat{I}_x + \hat{S}_y \hat{I}_y)$$

where $A_{||} = g_{||}\beta a_{||}$, $A_\perp = g_\perp \beta a_\perp$ (a – hyperfine splitting [mT]).

Spin Hamiltonian parameters of EMR spectra for samples containing Cu-Mn-Zn spinels supported on the NaY and HY zeolites (fresh samples) recorded at 293 K are given in Table 1. The value of hfs splitting $a_\perp$ could not be determined, because the hfs lines at the perpendicular orientation were poorly resolved. We have found that two types of Cu^{2+} complexes I and II exist in the cages of the HY zeolite. Since the spin Hamiltonian parameters fulfil the inequality $g_{||} > g_\perp > g_e = 2.0023$, the orbital ground state of the unpaired electron of Cu^{2+} cation for both complexes is $|x^2 - y^2>$. According to the Jahn–Teller effect, the Cu^{2+} complex I has the symmetry of tetragonally elongated *trans*-octahedron D_{4h}, and Cu^{2+} complex II has the symmetry of tetragonally distorted tetrahedron (pseudotetrahedron) D_{2d} [9].

In the EMR spectrum of Mn^{2+} complex, only six hfs components originating from the m_s $|-\frac{1}{2}> \rightarrow |+\frac{1}{2}>$ transition were observed (see Fig. 5). Other transitions of this type were not visible due to the overlapping of fine structure lines. Between the six hfs lines, we have observed small additional peaks that resulted from the forbidden transitions described by Bleaney *et al.* [10]. These lines appear under circumstances where the zero-field splitting (ZFS) has to be taken into account [11].

Spinels on the surface of the zeolites maintain their original spinel structure. However, some cat-

Table 1. Spin Hamiltonian parameters of EMR spectra (g factors, hyperfine splittings a [mT]) for samples containing Cu-Mn-Zn spinels supported on different zeolites (293 K)

Carrier	Loading [%]	Cu complex I			Cu complex II			Mn complex	
		$g_{||}$	$a_{||}$ [mT]	$g_\perp$	$g_{||}$	$a_{||}$ [mT]	$g_\perp$	g	a [mT]
NaY	10	2.355	12.3	2.055	–	–	–	–	–
HY	5	2.373	12.4	2.067	2.331	15.7	2.038	2.002	9.5
	10	2.373	12.5	2.065	2.331	15.6	2.037	2.001	9.6
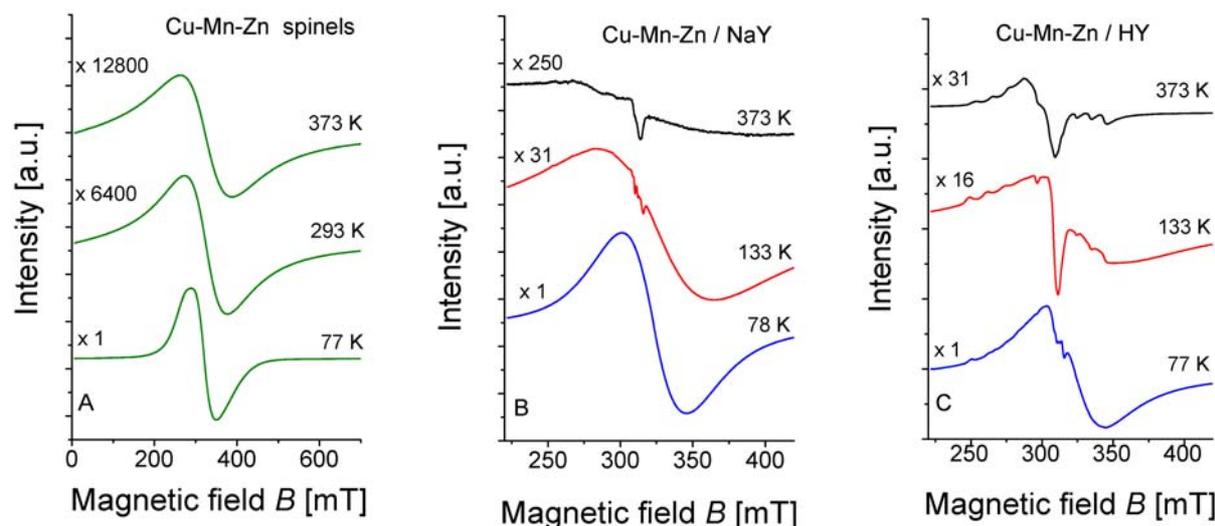
Fig. 3. Changes of EMR spectra with temperature: A – Cu-Mn-Zn spinels; B – Cu-Mn-Zn/NaY (10 wt%); C – Cu--Mn-Zn/HY (10 wt%).

ions originating from spinels bind to the surface of zeolites due to the ion-exchange Cu and/or Mn cations onto the cages of Y zeolite. Signals of $Cu^{2+}(I)$, $Cu^{2+}(II)$ and Mn^{2+} complexes are derived from cations located in exchangeable extra-lattice positions. No EMR lines from isolated Cu^{2+} and Mn^{2+} cations were observed in the EMR spectra of pure spinel. We have seen only a very single broad EMR line, which came from pure spinel phase (Fig. 3A). A comparison of the EMR spectrum of the bulk spinels with spinels supported on NaY and HY zeolites at 293 K shows that exchange interactions between electron spins in the bulk spinels were strongly reduced after loading them on zeolites. The decrease in the size of the crystallites inside the zeolite cages led to the reduction in the exchange interactions in spinels. The reduction in the exchange interactions was revealed by a significant reduction in the intensity of the EMR line.

We have studied the temperature dependence of EMR spectra for the investigated samples. Figure 3A shows the resonance spectra for antiferromagnetic Cu-Mn-Zn spinels in the temperature range between 77 and 373 K. It results from the aforementioned figure that the position of the resonance field B_{res} remains nearly constant with temperature, but the linewidth ΔB_{pp} strongly increases. It is worthy to notice that the resonance line intensity decreases with temperature.

EMR spectra of Cu-Mn-Zn/NaY and Cu-Mn--Zn/HY recorded at 77 K differ significantly from those recorded at 373 K. The EMR spectrum of Cu-Mn-Zn/NaY contains only one line attributed to Cu-Mn-Zn spinels (Fig. 3B). On the contrary, in the spectrum of Cu-Mn-Zn/HY sample, a smaller line from Cu^{2+} complex is observed, in addition to the broad line (Fig. 3C).

The intensity of the EMR lines recorded at 373 K for spinels supported on zeolites is very low, but it increases with decreasing temperature to 77 K. This effect is the most clearly seen in the case of NaY zeolite (Fig. 3B). It is worth noting that the value of resonance induction of magnetic field B_{res} is nearly constant (Fig. 4), as it was for pure spinels.
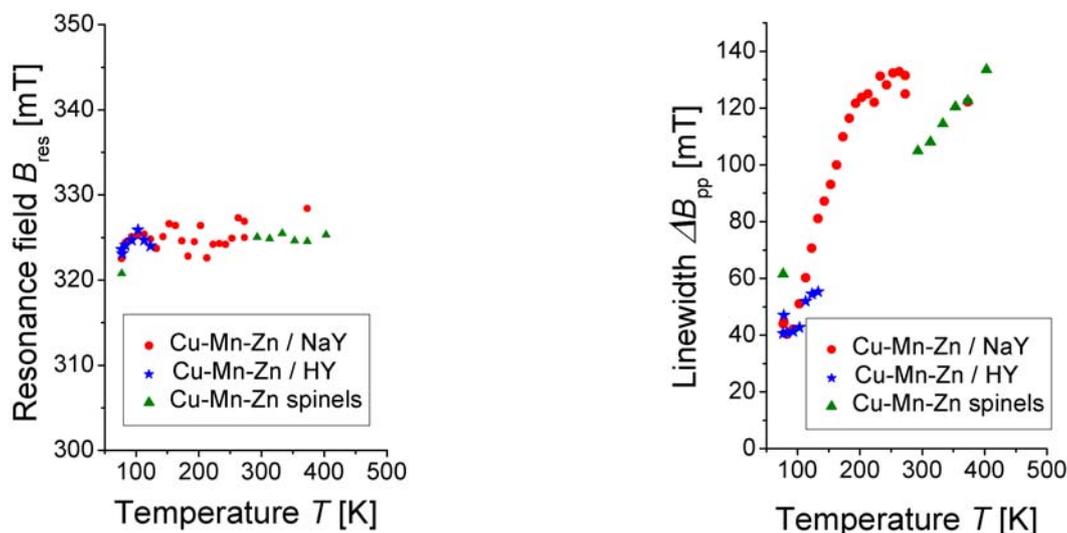
Fig. 4. Temperature dependence of resonance field B_{res} and linewidth ΔB_{pp} for Cu-Mn-Zn spinels, Cu-Mn-Zn/NaY (10 wt%) and Cu-Mn-Zn/HY (10 wt%).

The decrease in temperature leads to an increase of exchange interactions between electron spins and causes a reduction in the values of the EMR linewidth ΔB_{pp} (Fig. 4). The linewidth ΔB_{pp} of pure spinels was well determinable to 403 K, while the linewidth ΔB_{pp} of spinels on HY zeolite was only to 133 K. In the case of spinels supported on NaY zeolite, the linewidth ΔB_{pp} of resonance line was determined up to 273 K.

A comparison of the temperature dependence of EMR spectra of Cu-Mn-Zn spinels loaded onto NaY and HY zeolites shows that intensities of the EMR lines for the spinels in HY zeolite are weaker than those in NaY zeolite. It leads to the decrease of the exchange interactions between electron spins in the spinel. This points to a significant effect of the kind of aluminosilicate matrix on properties of Cu-Mn-Zn spinels. The interaction of Cu-Mn-Zn mixed oxides with zeolite HY is stronger than that with zeolite NaY (Fig. 3B and Fig. 3C).

The spin Hamiltonian parameters of Cu^{2+} and Mn^{2+} complexes did not change with temperature for both zeolites.

The samples Cu-Mn-Zn/NaY and Cu-Mn-Zn/HY were evacuated at different temperatures. The EMR spectra of evacuated samples recorded at room temperature did not show significant changes of the lineshape, the line intensity and the spin Hamiltonian parameters. In the case of samples heated and evacuated at 673 K, the intensity of EMR spectra was reduced, if recorded at 77 K (Fig. 5). This indicates that after the evacuation at 673 K, Cu-Mn-Zn spinels deposited on NaY and HY zeolites lost their stability. It is worth noting that for the sample Cu-Mn-Zn/NaY, the line intensity was reduced by one order of magnitude. This may suggest that Cu-Mn-Zn antifer-
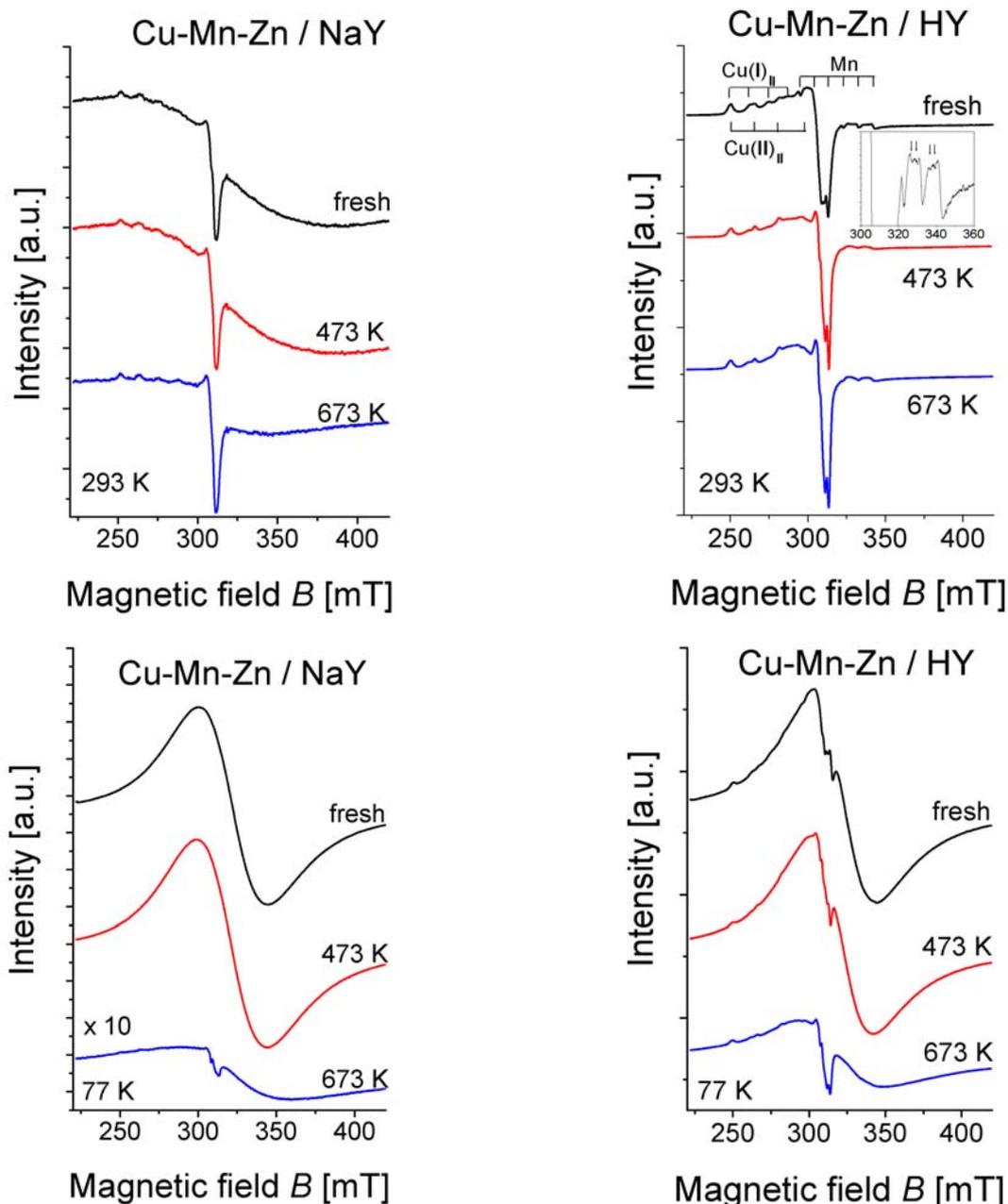
Fig. 5. EMR spectra of Cu-Mn-Zn/NaY (10 wt%) and Cu-Mn-Zn/HY (10 wt%) samples evacuated at different temperatures for 2 h recorded at 293 K and 77 K. The arrows in the inset show the forbidden transitions for ^{55}Mn.

romagnetic spinels on HY zeolite are more stable than those on NaY zeolite.

We believe that this phenomenon is caused by differences in the acid properties of the NaY and HY zeolites. FTIR measurements of samples with adsorbed pyridine have shown that the strength of acid centers on HY zeolite was much greater than that on NaY zeolite.

Conclusions

The study on the influence of Y type zeolites on EMR spectra of supported copper-manganese-zinc mixed oxide spinels have brought us the following conclusions.

The analysis of EMR spectra proved the occurrence of interactions between Cu-Mn-Zn spinels and NaY and HY zeolites. The results of EMR measurements point to the appearance of paramagnetic complexes containing Cu^{2+} and Mn^{2+} cations.

The type of zeolite (NaY or HY) determines the character of the EMR spectrum of the investigated samples. In EMR spectra of Cu-Mn-Zn/NaY and Cu-Mn-Zn/HY samples recorded at 293 K the presence of two Cu^{2+} complexes was observed (octahedral coordinated Cu^{2+}, as well as Cu^{2+} in pseudotetrahedral environment), whereas in the case of Cu-Mn-Zn/HY sample an additional signal coming from Mn^{2+} complex was recorded.

During the evacuation of all samples at 673 K, the signal intensity in the EMR spectra measured at 77 K was reduced. For Cu-Mn-Zn/NaY, this reduction was significantly greater than that for Cu-Mn-Zn/HY. It was proved that different strength of interactions between the zeolites and the Cu-Mn-Zn spinels results from differences in the acidity of NaY and HY zeolites.

References

1. Fierro, G., Morpurgo, S., Lo Jacono, M., Inversi, M., & Pettiti, I. (1998). Preparation, characterisation and catalytic activity of Cu-Zn-based manganites obtained from carbonate precursors. *Appl. Catal. A-Gen.*, *166*(2), 407–417. DOI: 10.1016/S0926-860X(97)00283-4.

2. Fei, J. H., Yang, M. X., Hou, Z. Y., & Zheng, X. M. (2004). Effect of the addition of manganese and zinc on the properties of copper-based catalyst for the synthesis of syngas to dimethyl ether. *Energy Fuels*, *18*(5), 1584–1587. DOI: 10.1021/ef049961f.

3. Fei, J. H., Hou, Z. Y., Zhu, B., Lou, H., & Zheng, X. M. (2006). Synthesis of dimethyl ether (DME) on modified HY zeolite and modified HY zeolite-supported Cu-Mn-Zn catalysts. *Appl. Catal. A-Gen.*, *304*, 49–54. DOI: 10.1016/j.apcata.2006.02.019.

4. Padlyak, B. V., Wojtowicz, W., Adamiv, V. T., Burak, Ya. V., & Teslyuk, I. M. (2010). EPR spectroscopy of the Mn^{2+} and Cu^{2+} centres on lithium and potassium-lithium tetraborate glasses. *Acta Phys. Pol. A*, *117*(1), 122–125.

5. Guskos, N., Glenis, S., Typek, J., Żołnierkiewicz, G., Berczyński, P., Wardal, K., Guskos, A., Sibera, D., Moszyński, D., Łojkowski, W., & Narkiewicz, U. (2012). Magnetic properties of $ZnFe_2O_4$ nanoparticles. *Cent. Eur. J. Phys. 10*(2), 470–477. DOI: 10.2478/s11534-012-0013-3.

6. Zapotoczny, B., Dudek, M. R., Guskos, N., Kozioł, J. J., Padlyak, B. V., Kośmider, M., & Rysiakiewicz-Pasek, E. (2012). FMR study of the porous silicate glasses with Fe_3O_4 magnetic nanoparticles fillers. *J. Nanomater.*, *2012*, article ID 341073(7pp.). DOI: 10.1155/2012/341073.

7. Jiang, M., & Karge, H. G. (1995). FTIR study of the kinetics of solid-state ion exchange in zeolites using pyridine as a probe. *J. Chem. Soc. Faraday Trans.*, *91*(12), 1845–1851. DOI: 10.1039/ft9959101845.

8. Karge, H. G., Hunger, M., & Beyer, H. K. (1999). Characterization of zeolites – infrared and nuclear magnetic resonance spectroscopy and X-ray diffraction. In J. Weitkamp & L. Puppe (Eds.), *Catalysis and zeolites: Fundamentals and applications* (pp. 198–326). Berlin: Springer-Verlag.

9. Goslar, J., & Więckowski, A. B. (1985). Migration and structure of aqueous Cu^{2+} complexes in Faujasite. *J. Solid State Chem.*, *56*(1), 101–115. DOI: 10.1016/0022-4596(85)90257-9.

10. Bleaney, B., & Rubins, R. S. (1961). Explanation of some 'forbidden' transitions in paramagnetic resonance. *Proc. Phys. Soc.*, *77*(1), 103–112. DOI: 10.1088/0370-1328/77/1/312.

11. Lender, Z., Goldfarb, D., & Batista, J. (1993). Magnetic resonance studies of SAPO-44 and MnAPSO-44. *J. Am. Chem. Soc.*, *115*(3), 1106–1114. DOI: 10.1021/ja00056a040.